

## 5. Materials and Methods

---

### 5.1. Introduction.

A series of questions were posed at the end of Chapter 2. The main research question was “**In the context of pottery, how is cuisine implicated in the changes that took place at the transition to agriculture, c. 4200-3900 B.C?**” A sequence of practical sub-questions was outlined according to those where answers must be established before the questioning could continue. The first three questions deal with establishing the presence of food indicators. Background research has shown that lipid residue analysis, starch, phytolith and calcium oxalate analysis are all potential ways of extracting and characterising evidence of former ceramic use.

All of the carbonised deposits were subjected to low-powered microscopic analysis, and section 5.2 details the protocol followed. Section 5.3 outlines the lipid residue analyses carried out to ascertain the animal food contents of the vessels. In section 5.4 the materials and methods used to answer these three sub-questions are outlined for the plant microfossils, namely starches, phytoliths and calcium oxalates:

- *Do indicators of foods (phytoliths, starches, calcium oxalates) survive in association with Ertebølle and Funnel Beaker ceramics from the sites chosen for investigation?*
- *Are these indicators related to the vessel use or are they derived from the burial environment?*
- *If food indicators do survive can they be used to characterise the products that were used in the pots?*

In section 5.5 we discuss some experimental work done to replicate the characteristics of residues. These replications provided many of the modern reference specimens for bulk isotope analysis and the charred plant foodcrusts.

### 5.2. Low powered microscopy.

All 114 surface deposits were investigated microscopically at low-power using a Wild M3 Heerbrugg reflective microscope. The microscope was equipped with a QImaging Camera version 6.3 (*Media Cybernetics Inc.*), linked to the digital

imaging programme Image Pro Plus. Low powered microscopy constituted the primary stage of investigation before the surface deposits were split for lipid residue analyses and plant microfossil analyses respectively.

Samples were laid on sterile foil and comprehensively scanned in grid transects at a magnification of x10 for visible remains including plant matter, bone fragments and pieces of fish scale. Higher magnifications of x40 were used to take more detailed images of objects. Any preserved remains were removed to eppendorf tubes for storage and identification.

### **5.3. Lipid residue analysis.**

The analyses are part of the researches of the ‘Baltic Foragers and Early Farmers Ceramic Research Project’, which is a collaborative venture between the Universities of York and Bradford. Whilst surface deposit residues were investigated at York for plant microfossils, both these residues *and* absorbed residues in the sherd fabric were analysed for lipid contributions at the Bradford AGES laboratories.

All lipid residue analyses were carried out by Dr. Val Steele at the University of Bradford, in conjunction with Professor Carl Heron (University of Bradford) and Dr. Oliver Craig (University of York). After extraction of the lipids, the extracts were prepared and run on a Gas Chromatograph (GC), Gas Chromatograph –Mass Spectrometer (GC-MS), and Gas Chromatograph-Combustion-Isotope Ratio Mass Spectrometer. GC and GC-MS analysis was carried out at the AGES laboratories at the University of Bradford. GC-C-IRMS samples were run at the isotope laboratories at the University of Newcastle.

Full Standard Operating Procedures including health and safety considerations for the methods involved were produced by Dr. Val Steele, and are included in Appendix II Also included is a short report on the methodology adopted for analyses.

#### **5.3.1. Modern reference material.**

Details of the experimental cooking with replica Ertebølle and Funnel Beaker vessels are given in Section 5.6 of this chapter. As well as providing insight into the conditions for successful processing and cooking of a range of animal and plant

foods using traditional techniques, these investigations also produced absorbed and surface residues useful as bulk isotope references.

## **5.4. Plant microfossils.**

Systematic retrieval of plant microfossil evidence was carried out by the author at the BioAch facilities, University of York using *only* the charred surface deposits. The recovery of starch was focused on, with some preliminary trials in phytolith recovery made too. Incidental recovery of calcium oxalate crystals was carried out. Automated classification of starches using an image recognition programme was done in collaboration with Dr. Julie Wilson from the Department of Chemistry and Complex Systems at York University.

### **5.4.1. Starch reference plants.**

Twelve modern reference species were selected on the basis of their occurrence as macrofossils on later prehistoric sites in northern Europe, their availability, and their potential value as a starchy food in prehistory. Domesticated cereals are represented by einkorn (*Triticum monococcum*), whilst hazelnuts (*Corylus avellana*) and acorns (*Quercus sp.*) are of suggested importance as wild staples (Holst, 2010; Kubiak-Martens, 1999; Mason, 2000). Other species included were edible reed types (*Acorus calamus*, *Cyperus longus*, *Typha latifolia*, *Sparganium erectum*), lords-and-ladies tuber (*Arum maculatum*), bracken fiddlehead (*Pteridium sp.*), root of wild horseradish (*Armoracia rusticana*) and meadowsweet (*Filipendula ulmaria*), and beechnut (*Fagus sp.*).

Harvesting from the wild was executed with sustainability in mind. Plants were collected where land access was permissible. Only a small portion of the root mass was removed to make the starch collection, so the plant was not destroyed. Fruiting bodies, leafy material and nuts were responsibly collected, leaving enough to sustain the wild animals that rely on them.

Plant specimens were identified by the author, and verified by Dr. Allan Hall (University of York). Collection was ongoing from May 2009 to September 2010. A number of specimens were provided by The Royal Botanical Gardens at Kew, London. Others were acquired from nurseries. Descriptions of modern reference starches are recorded in Appendix III.

Fresh starch specimens were prepared by peeling the underground storage organ and cleaning in UltraPure water. The specimen was rubbed against a clean, labelled slide and mounted in glycerol. In some cases where the lipid content of the specimen was high, crushing of the sample in a clean pestle and mortar was necessary to separate the starches from the lipid rich matter. Dried samples were also crushed and a small quantity mounted in glycerol. Multiple slides allowed some of the intra-population variability in starch morphology to be represented. These variations depend on such factors as season of procurement, the position of the sample in the plant, and age of the plant.

#### 5.4.2. Phytolith reference material.

Specimens destined for phytolith reference material were weighed then sonicated three times for 5 minutes in UltraPure water with water changes between each sonication episode. This was to remove phytolith contaminants that had been airborne and adhered to the plant exterior. Approximately a kilogram of fresh weight was collected of each specimen so that variation based on plant maturity, silica content of soil, and micro-environmental effects to the transpiration system could be accounted for and represented (Marco Madella *pers. comm.*). To a certain extent leaf matter and herbaceous plants were focused on because this is an area where starches are deficient. Samples were then dried at 100°C, before being furnace to ash at 450°C for 2 hours. A known amount of the ash was mounted on a clean, labelled slide in glycerol in a single plane.

Common name	Latin name
Hawthorn	<i>Crataegus monogyana</i>
Dog rose	<i>Rosa canina</i>
Borage	<i>Borago officinalis</i>
Rosebay willowherb	<i>Epilobium angustifolium</i>
Greater plantain	<i>Plantago major</i>
Crab apple	<i>Malus sylvestris</i>
Dandelion	<i>Taraxacum officinalis</i>
Wheat	<i>Triticum dicoccum</i>
Clover	<i>Trifolium repens</i>
Waterlily	<i>Nuphar lutea</i>
Lovage	<i>Levisticum officinale</i>
Sorrel	<i>Rumex acetosa</i>

<b>Fennel</b>	<i>Foeniculum vulgare</i>
<b>Chamomile</b>	<i>Anthemis arvensis</i>
<b>Salsify</b>	<i>Tragopogon porrifolius</i>
<b>Rowan</b>	<i>Sorbus aucuparia</i>
<b>Strawberry</b>	<i>Fragaria vesca</i>
<b>Nettle</b>	<i>Urtica dioica</i>
<b>Sloe</b>	<i>Prunus spinosa</i>
<b>Blackberry</b>	<i>Rubus fruticosus</i>
<b>Elderberry</b>	<i>Sambucus nigra</i>

**Figure 5. 1. A table listing the modern plant reference species incorporated into the phytolith reference collection.**

The species chosen for the phytolith reference collection are shown in figure 5.1. A table illustrating those specimens that were useful for their starch content, and those that were exploited for their silica content is given in Appendix IV. The presence of the different morphologies of calcium oxalate crystal was also noted. Although the reference collection is not exhaustive, it does represent a large number of edible species native to temperate Europe, and can be considered comprehensive of the main exploitable plant resources. Images and descriptions of modern phytolith and calcium oxalate references is given in Appendix V, as is a table summarising the complete starch, phytolith and calcium oxalate content of all the modern plants studied in comparison to each other.

#### **5.4.3. Experimental foodcrusts.**

In order to test whether starches and phytoliths survive the cooking process, einkorn (*Triticum monococcum*) and acorn (*Quercus sp.*) were boiled in water for 3h in replica ceramic vessels (figure 5.2). During the experiment spot temperatures were recorded with a thermocouple at regular intervals both in the liquid and on the surface of the pot. After boiling the pots were air dried and the experiment was repeated 3 times. Foodcrust rapidly accumulated on the inside of the vessels, to a thickness of up to 5mm (figure 5.2). The pots were air dried and sealed in plastic bags for further analysis.



**Figure 5. 2.** The image on the left shows the cooking experiments in progress. The image on the right shows the resulting carbonised foodcrust in the base of a TRB replica vessel after cooking.

#### **5.4.4. Starch and Phytolith Extraction.**

Carbonised residues (<1mg) from experimental and archaeological vessels were removed with a scalpel and accurately weighed into sterile plastic tubes and treated with hydrogen peroxide ( $H_2O_2$ ; 10%, 10ml; 15-30 min), whilst gently disaggregating the carbonised matrix with a spatula. The tubes were centrifuged (3000rpm; 3 min) and the supernatant removed, the remaining residue was washed three times with UltraPure water and made up to a 1ml suspension in UltraPure water. Particulate matter was allowed to separate and the remaining supernatant, containing liberated starch granules, phytoliths and calcium oxalate crystals, was added to glass microscope slides which were then left to dry at room temperature. Dried samples were mounted in a single plane in glycerol and left at room temperature for at least 24h before viewing.

This is an adaptation of the methodology employed by Zarillo *et al.* (2008), and uses a slightly higher concentration of hydrogen peroxide, but leaves out the heavy liquid density separation with Sodium Polytungstate ( $Na_6(H_2W_{12}O_{40})$ ). The reason for this is that heavy liquid separation targets starches of a specific gravity of  $\sim 1.5$ , but insufficient research has been done on changes to specific gravity caused by heat alteration. Retrogradation is known to alter molecular organisation by adding and removing amylose polymers, which changes the molecular weight and the density of the granules (Sajilata *et al.* 2006). This could potentially alter their specific gravity and cause them to be removed. Removal of the heavy-density liquid separation, and

replacement with a procedure that repeatedly adds starch-rich supernatant to the slide was found to be inclusive of all forms of starches, and also phytoliths in a simpler procedure.

#### **5.4.5. Amylase degradation.**

To confirm their presence, starch was re-extracted from a selection of the archaeological samples and two equal aliquots (1ml), were added to wells of a 12-well polystyrene tissue culture plate (*Fisher Scientific, UK*). Two aliquots of starch powder (1ml; 150 mg ml<sup>-1</sup>; *Zea mays, commercially available*) were also added to wells on the plate to provide a positive control. Thermally-stable  $\alpha$ -amylase (0.25ml; undiluted, *Sigma, UK*) was added to one set of wells containing each archaeological and control extract. Ultra-pure water, containing no enzyme, was added to the other set to serve as a control. The plates were incubated at for 24 hours at 25°C. The contents of each well was then mounted in a single plane in glycerol and left at room temperature for at least 24h before viewing.

#### **5.4.6. Microscopy.**

Polarized and brightfield light microscopy observations of the microfossil extracts were performed with an Olympus IX71 inverted microscope (*Olympus, UK*) fitted with a ColorView III microscope camera (*Olympus, UK*) linked to the Digital Image Solutions program CellD, version 2.6 (Build 1200) (*Olympus, UK*). A grid (200 $\mu$ m) was imposed over the slide and all the starches and phytoliths on the slide were counted.

#### **5.4.7. Investigating contamination from the burial environment.**

In order to be confident that the microfossils were not background loading from the burial environment samples of deposits from interior (F) and exterior (S) surfaces (figure 5.3) were compared for the number of starches and phytoliths they contained mg<sup>-1</sup>. This was further compared to soil samples where they were available from Neustadt. Soil samples were prepared using the same extraction procedure. Five soil samples were analysed (mean 276.5 mg).



**Figure 5. 3. Left, sherd 3020 from Neustadt showing the interior deposit (F). Right, the same sherd showing the exterior sooty deposit (S).**

Hypothetically, interior (F) deposits should contain more plant microfossils than exterior (S) deposits if the pots had been deliberately packed with plants. Ideally a two sample single-tailed t-test should establish a statistically significant difference between (F) and (S). However, it was noted that on some sites where plant processing seemed to be less important overall, the small number of (F) deposits that show high counts would not be deemed viable for further investigation because they had not contributed enough to establish the (F) cluster's significance. In this case, the small numbers of pots representing plant processing are archaeologically significant, and so it was important not to exclude them.

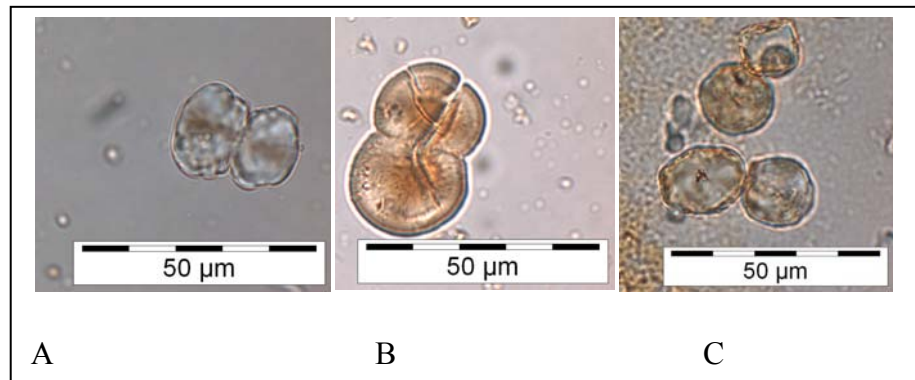
In cases where there was not a significant difference between (F) and (S) a less ideal measure was taken to test the significance between observationally high and low clusters. This approach not only allowed for the inclusion of those archaeologically significant samples where plants were processed on otherwise devoid sites, but it also allowed for the inclusion of a minor number of (S) deposits that had high counts. These were almost certainly the result of overspill from the interior contents of the pots, as most of these instances occur at the rim. Samples with counts  $\text{mg}^{-1}$  below a defined threshold value for that site were removed from subsequent analysis by automated classification in the case of starches, or measurement and description in the case of phytoliths.

#### **5.4.8. Image acquisition for automated starch classification.**

Starches that showed evidence for extensive heat alteration were not chosen for imaging. Through heating in water the extinction cross becomes progressively more visible before becoming diffuse at the edges of the grain, and the granule swells. One degradation pathway results in the rupture and gelatinisation of the granule, which is



beginning in figure 5.4a. The second taphonomic pathway evidenced by many of the granules is retrogradation, as for example those granules in figure 5.4b. In these instances swelling is slow enough that catastrophic structural changes do not take place. The partial loss of amylose and crystallization of the remainder renders the granules more brittle, and cracking can occur, usually along expanded lamellae.



**Figure 5.4.** A) A partially gelatinised starch granule that is losing its molecular order, B) A swollen granule that has become brittle from the leaching of amylose, C) Modern maize (*Zea mays*) starches after a tannin soak showing evidence of staining.

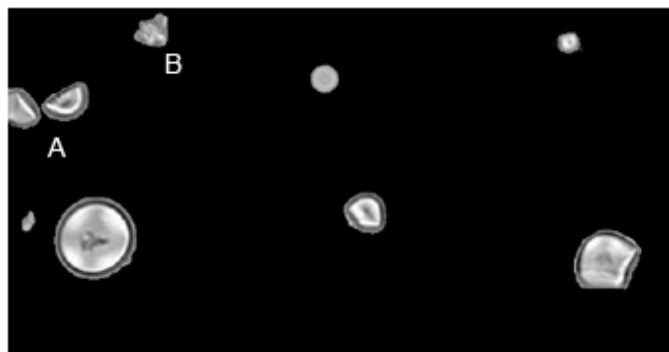
Other possible features of heat alteration or the burial environment include some staining. This occurs on both thermally unaltered and retrograded granules suggesting the staining itself is not damaging other morphological features, and simply represents a similar process as occurs with the addition of iodine (Torrence and Barton, 2006). When maize granules were soaked for forty-eight hours in oak tannins at 20°C, they were found to uptake the tannin stain without alteration to their extinction cross or size and shape characteristics (figure 5.4c). In selection of granules for classification therefore, granules were not dismissed if they were stained, but ones that displayed the least heat alteration in terms of retrogradation cracking and gelation were not selected for imaging.

Images of the starch grains were obtained at a resolution of 2576 x 1932 x 24bit bitmap (BMP). The magnification was set at x600. Images were taken in pairs, consisting of one photograph taken in brightfield and a corresponding photograph in polarised light. The number of images varied because of differences in the ease of extracting and cleanly mounting specimens, to reduce extraneous organic obscuration. Images were taken of modern fresh plant starches in order to train the programme on native temperate northern-European species. Similar pairs of images

were then taken of the archaeological specimens for pixel-resolution measures of consistency to the reference starch.

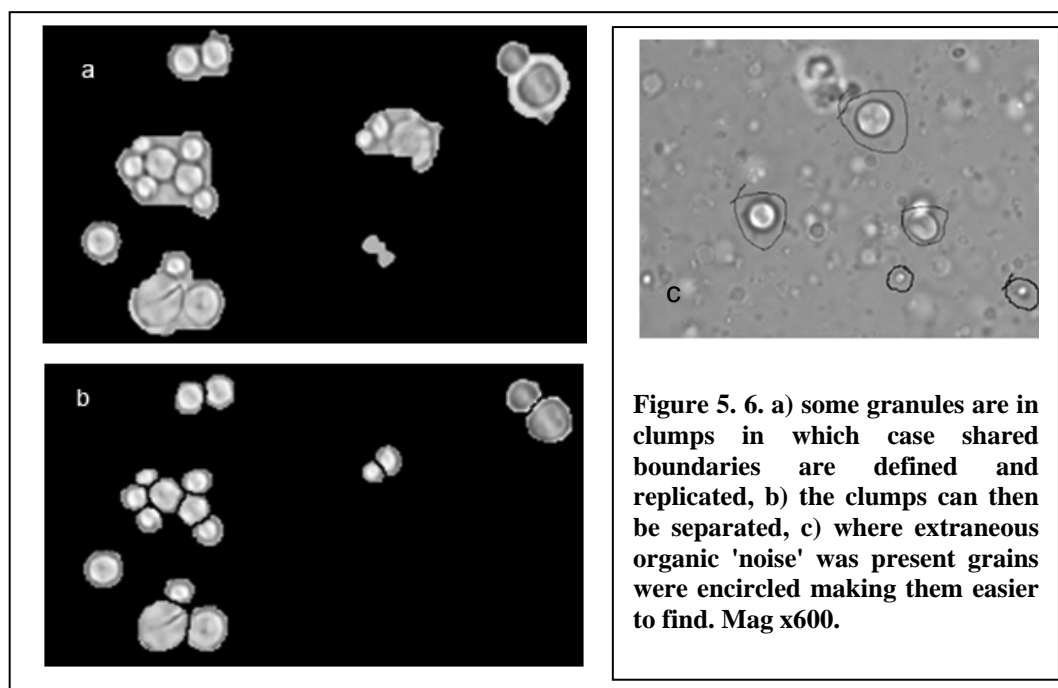
#### 5.4.9. Image analysis and starch classification.

In order to extract features for classification from both modern and ancient starches, the boundaries of individual grains were first identified in the images. Where possible this was achieved automatically using edge detection methods. Sudden changes in pixel intensity at the edges of objects allow their identification by analysis of the gradient, or rate of change of image intensity. Pixels with a gradient magnitude above a threshold based on the image's intensity statistics were used to define the boundaries of the objects. Any objects in contact with the edge of the image (e.g. Object A, figure 5.5) were deleted as they may not be full grains. Wilson *et al.* (2010) used shape descriptors, including a measure of concavity, to recognize and delete damaged granules. Such an automated process was always not possible here because shape descriptors are not able to distinguish between starches and some of the other organic matter seen in these images (e.g. Object B, figure 5.5). It was therefore necessary to visually identify and delete objects that were not starch grains.




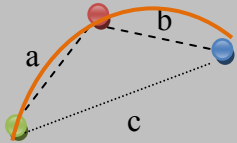
**Figure 5. 5. Objects automatically recognised by the programme could not be analysed if they were A) in contact with the edge of the image or, B) not starch granules. x600.**

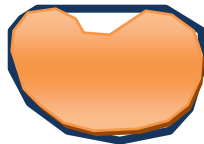
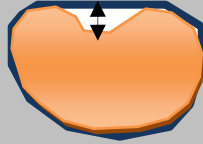
For some images, automated boundary recognition was followed up by manual separation of grains forming clumps with shared boundaries (figure 5.6 a & b). All manual intervention was performed using the software GraphicConverter (Lemkesoft GmbH). Where there was excessive background noise, rough circles were drawn around the grains to prevent other organic matter from forming objects. Thus the automated boundary recognition was deployed only within those circles, illustrated in figure 5.6 c. In the worst cases locating the granules was done by defining their boundary manually in GraphicConverter.



For each grain, a total of 26 feature variables were recorded for classification. Variables were calculated based on size and shape of the granule, its boundary curvature and concavity and the shape of its polarization cross. Detail on these variables is summarised in figure 5.7. In addition, statistical measures were calculated from pixel intensities within the grain for both the brightfield and polarized images and the gradient magnitudes. The data from the training set grains was used to train supervised learning algorithms. Four different classifiers were trained; a self-organising map (SOM), learning vector quantization (LVQ) and support vector machines (SVM), both (SVM\_linear) and with a radial basis function kernel (SVM\_RBF).

Feature being studied	Variable	Description of information obtained.
Size	Granule area	The number of pixels that a granule covers.
	Granule length	The greatest distance between boundary pixels.
	Granule width	Maximum distance orthogonal to the granule length.
Shape	Granule length to width ratio	The ratio of the greatest distance between boundary pixels to the maximal distance orthogonal to this.
	Minimum box area to	The minimum sized box

	granule area ratio.	<p>possible is placed to enclose the granule, like so:</p>  <p>The ratio of box area to granule area is recorded.</p>
	Squared boundary length to area ratio.	The length of the boundary as described by the number of pixels is squared. The ratio of this to the area of the granule is recorded.
	Variance in distance from boundary to centroid of granule.	The amount of variation within the values of distance from boundary to granule centre.
	Elliptic variance	The granule shape compared to an ellipse where the major and minor axes are equal to the length and width of the granule respectively.
<b>Curvature</b>	Overall straightness of boundary	The relationship between pixels was given vector direction details. The overall straightness was measured by coding for the recognition of repeats in the vector chain.
	Length of maximum straight section as fraction of boundary	The proportion of the overall boundary that is straight; represented as a fraction.
	Total curvature	<p>The straight-line distance between the preceding and proceeding boundary pixel is subtracted from the sum of the lengths of the central pixel to its preceding and proceeding pixel, like so:</p>  <p>So, <math>a+b-c</math></p>

		<p>“The difference between the straight-line distance between the two points and that along the boundary gives the curvature” (Wilson <i>et. al.</i> 2010, 599).</p>
	Total concavity	<p>The difference between the area of the granule and that of its convex hull, where the convex hull is the smallest convex polygon that contains all the pixels of the granule, like so:</p> 
	Maximum concavity	<p>The greatest distance between the granule boundary and the convex hull, indicated by the arrow, like so:</p> 
<b>Polarization cross</b>	Area of cross to granule area ratio	<p>The area of the polarization cross is measured by the percentage of pixels below a threshold of <math>\mu + 0.1\sigma</math>, where <math>\mu</math> and <math>\sigma</math> are the mean and standard deviation of the pixels in each granule. This is given as a ratio to the overall granule area.</p>
	Total curvature of the cross arms	<p>Crosses were skeletonized, or rendered in black and white. The principles described above to acquire a curvature were applied to the skeletonized</p>

		polarisation cross.
Distance from cross centre to centroid of granule		The length from the defined centre of the granule to the centre of the extinction cross.
Minimum angle between the cross arms.		The smallest angle of the polarised arms radiating from the extinction point.

**Figure 5. 7. A table summarising the features of the granules measured in order to classify them (after Wilson *et al.* 2010).**

Classification of the modern training data was used to assess the internal consistency (both sensitivity and specificity) of the individual classifiers as well as combinations of classifiers. The best classification system was then applied to a completely independent *test* set, an unused sub-set of the modern reference starches, to test the extrapolation of the results to unseen data for external validation, as a blind-test. The trained classifier was then applied to experimentally cooked examples of *Triticum monococcum* and acorn (*Quercus* sp.) to test classification after thermal alteration. Finally the classifier was applied to archaeological starches from carbonised surface deposits.

#### **5.4.10. Phytolith classification.**

The International Working Group on Phytolith Nomenclature's (IWGPN) criteria for the description of phytoliths was adopted, and is detailed extensively in Madella *et al.* (2005). Like the starches, size and shape characteristics play an important part in description, but the many diverse cellular origins of phytoliths in comparison to starches means there are many other characteristics to consider also. Texture and ornamentation play a key role in classification, which has precluded the use of computer-assisted phytolith analysis to date.

Investigations were made into the possibility of developing an image analysis programme with the Complex Systems Department at the University of York. However, the complicated 3-dimensional structure of phytoliths that needs to be described, in combination with surface architecture that can add another level of complexity, and the number of possible orientations the silica bodies can be arranged in has so far precluded their reduction to a quantifiable and manageable set of measurements. In addition, there is no way to digitally discriminate between silica skeletons, extraneous organic detritus and single phytoliths in an image. So,

phytolith analysis remains in the domain of manual measurement and classification based on visible descriptors.

According to the IWGPN guidelines, if there are no previous publications describing observed phytoliths, new names should be made up of a maximum of three descriptors (Madella *et al.* 2005). The first is the shape in the main visible orientation. The second is the texture and/or the orientation of the body. Finally, the third is the anatomical origin of the phytolith, to tissue or cellular source. This final criterion should be used only when the origin is beyond doubt.

### **5.5. Experimental replication.**

In the summer of 2009 a series of cooking experiments were carried out in Schleswig-Holstein, Germany. The purpose was dual: first to generate absorbed and surface residues of foods and food combinations so that investigations could be made of the bulk isotope composition of mixtures. The second purpose was to replicate the conditions for a successful culinary outcome using Mesolithic and Early Neolithic technologies. Figure 5.8 details the main replications performed using plant foods. A full inventory of replica ceramics used to cook modern reference foods is given in Appendix VI.

In short, the *actions* of simulated culinary enterprise contributed to an understanding of the *chaîne opératoire* of Mesolithic-Neolithic cuisines. Successful culinary outcomes are conditional upon certain limited inputs, and I would argue that only through replication is it really possible to fully appreciate the subtleties of those conditions for success. It also allows for an appreciation of the conditions for failure, or limited successes. From the creation of the vessels with their varying compositions and inorganic ingredients, to the selection, gathering and hunting of what to cook in them, through to the construction of the fire and maintenance of temperature, and into the consumption of the cuisines created; these experiments were an exercise in the observation of experiences as much as a means to generate measurable residue characteristics.



Foods cooked and process used	Illustration	Type of pot	Method
<p><b>POT NUMBER:2</b></p> <p><b>Repeated boiling of acorns.</b></p>		Ertebølle	<p>117g of acorns, collected in the previous October from Northamptonshire, were boiled in 750ml of water. This was repeated three times, with the removal of remaining contents after each episode. At the end of the final boiling the remaining acorns were crushed to be boiled in water for a final 2 hours.</p>
<p><b>POT NUMBER:6</b></p> <p><b>Repeated boiling of einkorn and water.</b></p>		Funnel Beaker	<p>250g einkorn, 44g wheat bran, 6g wheat chaff, and 750ml of water were boiled for one hour, before the contents of the pot were cleaned out. This was repeated for six cooking episodes. Einkorn and bran was shop bought, and the wheat chaff was collected during harvest from Yorkshire.</p>
<p><b>POT NUMBER:3</b></p> <p><b>Successive boiling of einkorn with milk, and nettles with blubber.</b></p>		Funnel Beaker	<p>The three cooking successions were:</p> <ul style="list-style-type: none"> <li>(i) 250g einkorn, 44g wheat bran, 6g wheat chaff, 750 mls milk</li> <li>(ii) 120g nettles, 1000 mls water</li> <li>(iii) c. 500g Seal blubber</li> </ul> <p>Each cooking episode was two hours long, and the contents were removed between each stage.</p> <p>The einkorn was purchased from a local health-food shop, as was the wheat bran. The wheat chaff was collected from Yorkshire to simulate poorly cleaned grains. Nettles were from the immediate environs of the experimental area. Seal blubber was kindly donated by the Leibnitz Institute of Marine Sciences at the University of Kiel.</p>
<p><b>POT NUMBER:1</b></p> <p><b>Repeated boiling of nettles with water.</b></p>		Ertebølle	<p>120g nettles (<i>Urtica dioica</i>) were boiled with 1000ml of water for one hour. This was repeated six times. An extra 500ml of water was added 30 minutes into the first cooking because of evaporation loss. Nettles were foraged from around the experiment area</p>

Figure 5. 8. A table showing the main experiments carried out to replicate cooking of plant foods in ceramics.



## 5.6. Methodology development and evaluation.

### 5.6.1. Results of automated starch classification: can these modern starches be identified to plant source?

#### 5.6.1.1. The training set.

The number of images taken of each modern plant species is shown in figure 5.9. Each species was allocated a class number (figure 5.9, column 1), as a shorthand referent. The total number of granules about which features were acquired is given, and in most cases is well over 100. The training set and the test set are both sub-samples of the total number of granules.

Class #	Species	Common name	# Images	#Granules	#Training	#Test
1	<i>Acorus calamus</i>	Sweet flag	6	611	100	511
2	<i>Arum maculatum</i>	Lords-and-Ladies	6	265	100	165
3	<i>Cyperus longus</i>	Galingale	6	89	50	39
4	<i>Armoracia rusticana</i>	Horseradish	6	63	50	13
5	<i>Triticum monococcum</i>	Einkorn	6	149	100	49
6	<i>Pteridium</i> sp.	Bracken	5	255	100	155
7	<i>Filipendula ulmaria</i>	Meadowsweet	6	191	100	91
8	<i>Quercus</i> sp.	Oak (acorn)	8	40	30	10
9	<i>Typha latifolia</i>	Reedmace	6	344	100	244
10	<i>Fagus</i> sp.	Beech (beechnut)	6	222	100	122
11	<i>Sparganium erectum</i>	Bur-reed	6	71	50	21
12	<i>Corylus avellana</i>	Hazel (hazelnut)	5	653	100	553
<b>Total</b>			72	2953	980	1973

**Figure 5. 9. A table showing the modern plant references with their class number and details of the number of images, and granule number in training and test data sets.**

The best results on the training set were obtained from a single classifier called the SVM\_RBF classifier. Each cell in the figure 5.10 shows the percentage of granules of the species corresponding to the column label that were classified as the species corresponding to the row label. For example 92% of Class 1 (*Acorus calamus*) granules in the training set were correctly classified, but 8% were assigned to Class 7 (*Filipendula ulmaria*). Thus the cells on the diagonal show the percentages of correctly classified grains for each species.

As well as the 92% of Class 1 granules correctly classified as *Acorus calamus*, 1% of each of Class 2 (*Arum maculatum*), Class 6 (*Pteridium* sp.) and Class 9 (*Typha latifolia*), and 2% of Class 7 (*Filipendula ulmaria*) were also assigned to Class 1.. Specificity is a measure of not only the proportion of grains for a particular species that will correctly classify, but also the proportion of starches from other storage organs that will *also* incorrectly classify to that particular species. Specificity can then be used to improve the classification of further samples. For example, although the percentage of correctly classified grains is high for both *Acorus calamus* at 92% and *Corylus avellana* at 87%, more grains from other species are also classed as *Corylus avellana* whereas few granules are incorrectly classed as *Acorus calamus*. The specificity of the classifier for each species is given in the final row of figure 5.10. Since the specificity, as well as the sensitivity for *Acorus calamus* and *Quercus* sp. is high, granules classified as these species are more likely to be correct. In general, high specificity and sensitivity is found for all of the species in the reference collection.

	1	2	3	4	5	6	7	8	9	10	11	12
1	92	0	0	0	0	0	8	0	0	0	0	0
2	1	72	1	0	9	6	1	0	4	0	1	5
3	0	10	66	0	10	2	2	0	2	2	0	6
4	0	2	0	92	0	0	0	0	2	0	0	4
5	0	8	1	0	74	3	1	0	7	2	1	3
6	1	2	2	0	1	84	3	0	2	1	3	1
7	2	0	0	0	3	2	90	0	0	0	1	2
8	0	0	0	0	0	0	0	100	0	0	0	0
9	1	2	0	2	5	2	1	0	74	5	0	8
10	0	0	0	0	2	0	1	0	3	89	2	3
11	0	8	0	0	4	0	0	0	2	4	80	2
12	0	0	0	0	4	2	0	0	2	5	0	87
specificity	0.95	0.77	0.89	0.96	0.70	0.84	0.85	1.00	0.78	0.85	0.83	0.76

Figure 5. 10. A table showing the percentage of granules from the training set (first column), that were correctly classified to the corresponding class in the rows.

### 5.6.1.2. The Test Set.

The SVM\_RBF classifier was used to classify the individual granules in the test set (those granules not used during training). The results are shown in figure 5.11. Although there are very few acorn granules in total, all those in the test set are classified correctly due to their distinctive shape. *Acorus calamus* granules also classify well, with 81% of the 511 granules in the test classified correctly. The classification of individual granules for other species is less successful compared to the training set data. It may be that the classification of *Armoracia rusticana* and *Sparganium erectum* could be improved by increasing the number of training granules. These rates of correct classification are considerably and consistently higher than those obtained from primary testing of the programme on modern economic plants (Wilson *et al.* 2010). The highest correct classification rate was 79% for potato (*Solanum tuberosum*), but only 44% (4/9) of the plants studied were correctly classified in over half the instances. This is low compared to the reference plants in the present study; in 92% of plants (11/12) the rate of correct classification was >50%.

	1	2	3	4	5	6	7	8	9	10	11	12
1	81	0	0	1	0	7	9	0	0	1	1	1
2	0	50	2	4	20	4	2	0	6	1	1	11
3	0	11	53	5	18	5	3	0	3	0	0	3
4	0	0	8	58	8	0	17	0	0	0	0	8
5	0	6	2	0	65	0	2	0	18	0	2	4
6	2	8	1	2	8	61	1	0	5	3	5	4
7	12	2	2	4	2	6	66	0	1	0	0	3
8	0	0	0	0	0	0	0	100	0	0	0	0
9	1	5	0	1	9	4	0	0	67	5	2	7
10	3	0	0	0	3	3	6	0	3	69	2	12
11	5	5	0	0	20	10	5	0	5	5	45	0
12	1	5	0	1	6	3	3	0	3	8	3	66

**Figure 5. 11. A table showing the percentage of correctly classified granules using a set of modern starches (test set) not used to train the programme.**

The trained classifier was then used to classify multiple grains from a particular species. This was achieved by combining the classification of the individual test set grains within an image. The number of grains classified to a particular species in

each image was multiplied by the specificity for that species as determined on the training data (final row figure 5.10) to give a score for that species. If all classifiers were used, this allowed for a slight improvement in the results with a more accurate combined score. These results are shown in figure 5.12. The scores were ranked and the species with the highest score was then taken as the classification for that image.

Figure 5.12 also shows the number of misclassified images with the class number(s) that they were assigned to in brackets. The final column shows the rank of the correct class. Of the 67 images containing test set grains, 60 were classified correctly and, in all cases the correct class of the image appeared in the top 3 highest scores. Whilst individual granules from most species do not classify particularly well, classification of a collection of granules is much more successful. This can be explained by the fact that, with the exception of acorn here, most species have some round granules of a similar size with no particular discriminatory features. It would not be possible to classify these granules *individually* using any method. However, most of the species in this study do also have granules with distinctive features that allow the images to be classified correctly.

<b>Class</b>	<b>Species</b>	<b># images</b>	<b># correct</b>	<b># wrong(class)</b>	<b>Real class position</b>
<b>1</b>	<i>Acorus calamus</i>	6	5	1 (7)	2nd
<b>2</b>	<i>Arum maculatum</i>	6	6	0	-
<b>3</b>	<i>Cyperus longus</i>	5	5	0	-
<b>4</b>	<i>Armoracia rusticana</i>	6	5	1 (1)	3rd
<b>5</b>	<i>Triticum monococcum</i>	6	6	0	-
<b>6</b>	<i>Pteridium</i> sp.	5	5	0	-
<b>7</b>	<i>Filipendula ulmaria</i>	6	5	1 (1)	2nd
<b>8</b>	<i>Quercus</i> sp.	4	4	0	-

9	<i>Typha latifolia</i>	6	6	0	-
10	<i>Fagus</i> sp.	6	5	1 (12)	3rd
11	<i>Sparganium erectum</i>	6	3	3 (5, 9,10)	3rd, 3rd, 2nd
12	<i>Corylus avellana</i>	5	5	0	-

Figure 5. 12. A table showing the number of modern reference images that were correctly classified and the number that weren't as well as an overall ranking of that class.

### 5.6.1.3. Experimentally cooked residues.

When applied to the modern cooked einkorn (*Triticum monococcum*) and acorn (*Quercus* sp.) the trained SVM\_RBF classifier displayed mixed success. Although 87% of the 158 grains extracted for acorn were classified correctly, none of the cooked einkorn grains could be correctly identified. Our experimentally cooked einkorn starches were rendered 'bagel-shaped' (figure 5.13) by heat alteration. The small B-type grains from einkorn (*Triticum monococcum*) were barely recognisable as starch, being considerably blackened and dehydrated (figure 5.13).

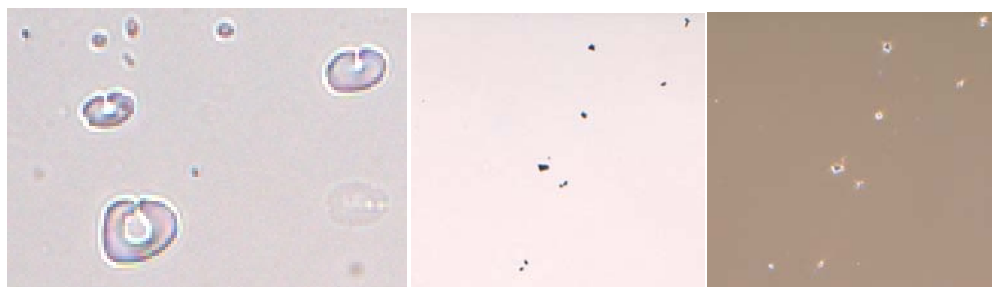


Figure 5. 13. On the left, an image of the degradation to einkorn (*Triticum monococcum*) A-type grains. In the middle and right, Type B grains are blackened in brightfield but retain an extinction cross in polarised light, all x600.

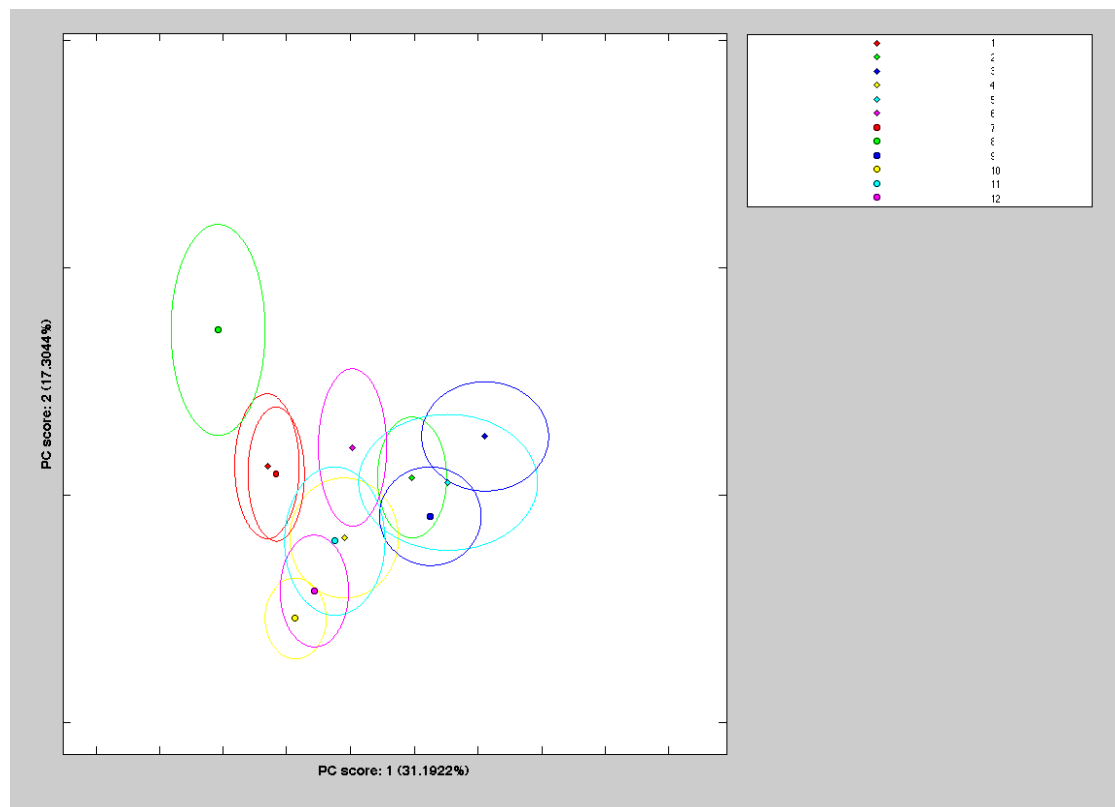
### 5.6.1.4. Evaluating the classifications.

Part of the reason for a poor preservation of cereal starch grains after cooking is likely a low amylose proportion of 25.0-27.4% (Frederiksson *et al.* 1998) that may not be enough to offset the alteration potential of temperatures that formed the archaeological foodcrusts. The characteristic bimodal distribution of starch types and morphologies in cereals may also be having an effect on the results, with large type A grains degrading very differently compared to smaller type B grains. Type-B grains have a higher amylose content which explains why they survive in higher

*numbers* than the larger Type-A grains. The extremely altered character of the B-type made it difficult for the automated classification to recognise them as starches though, so they did not contribute to the results. Because of this results that are built on *populations* of starches in a collection of images (figure 5.12) will be less likely to classify to a bimodal species than a class with only one modality.

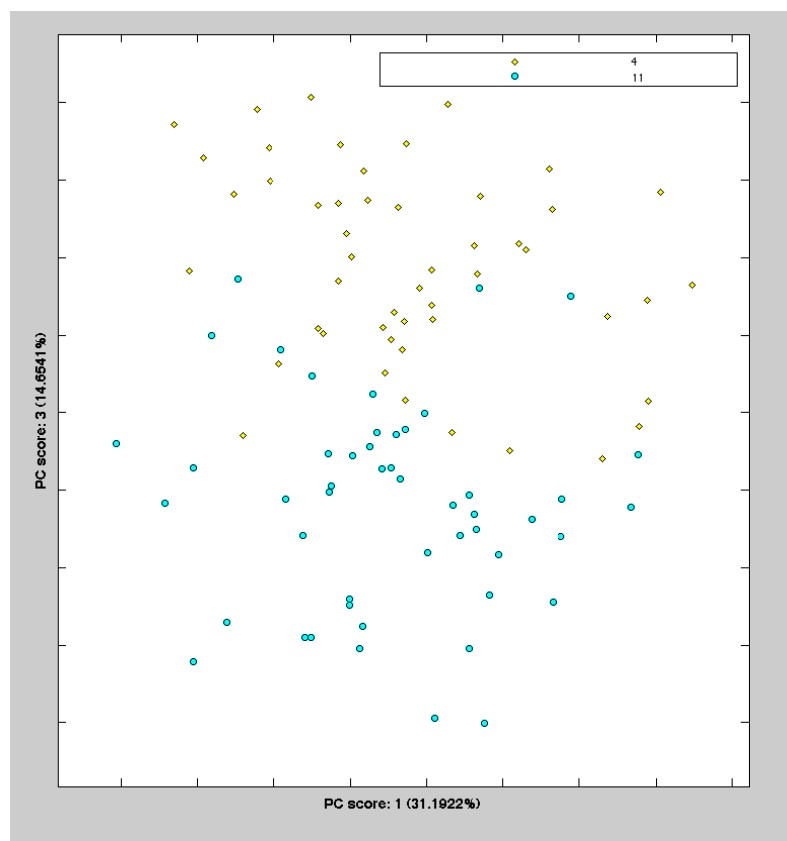
This limitation stems from the fact that the programme will always allocate a grain to its nearest category, acceptable if the starches being observed are from highly diagnostic populations, but with greater potential for error if they are not. However, what this means is that the more the programme is added to, the more accurate it becomes. In the future the programme will be trained on experimentally cooked starch populations to account for heat alteration more accurately. Having manually counted and observed all the archaeological grains however, there were no examples of starches that appeared ‘bagel-shaped’ or shrunken and blackened like the Type-B grains, so the likelihood that we are overlooking archaeological cereal grains because of our classification methodology is low. In addition, some of the speculated uses of cereals in prehistoric pottery as alcoholic beverages (Dineley and Dineley, 2000) do not involve high-temperature preparation, but can leave a residue.

As another measure of the degree to which the starches in the reference material are diagnostic of their species principal components analysis is a useful tool. Using a sample of 50 large granules for each class (30 in the case of acorn) figure 5.14 shows the first two principal components. Those with the most defined clustering and separation belong to *Quercus* sp., with some overlap of the other classes.



**Figure 5. 14. Principal components analysis of the modern starch references shows that using the first two principal components there is some clustering in classes.**

The mean score for each species along with a plotted standard deviation ellipse illustrates the areas of overlap between the species. Some groups such as 4 and 11 cannot be separated using the first two principal components. These groups can be separated when a third principal component is involved though. As figure 5.15 shows for example, principal component 1 and 3 separate *Azorella rusticana* (4) and *Sparganium erectum* (11). Based on multivariate statistical analyses and the measures of specificity and sensitivity the automated classification based on 26 morphological *is* representing statistically measurable differences that *do* separate the classes in the modern reference list.



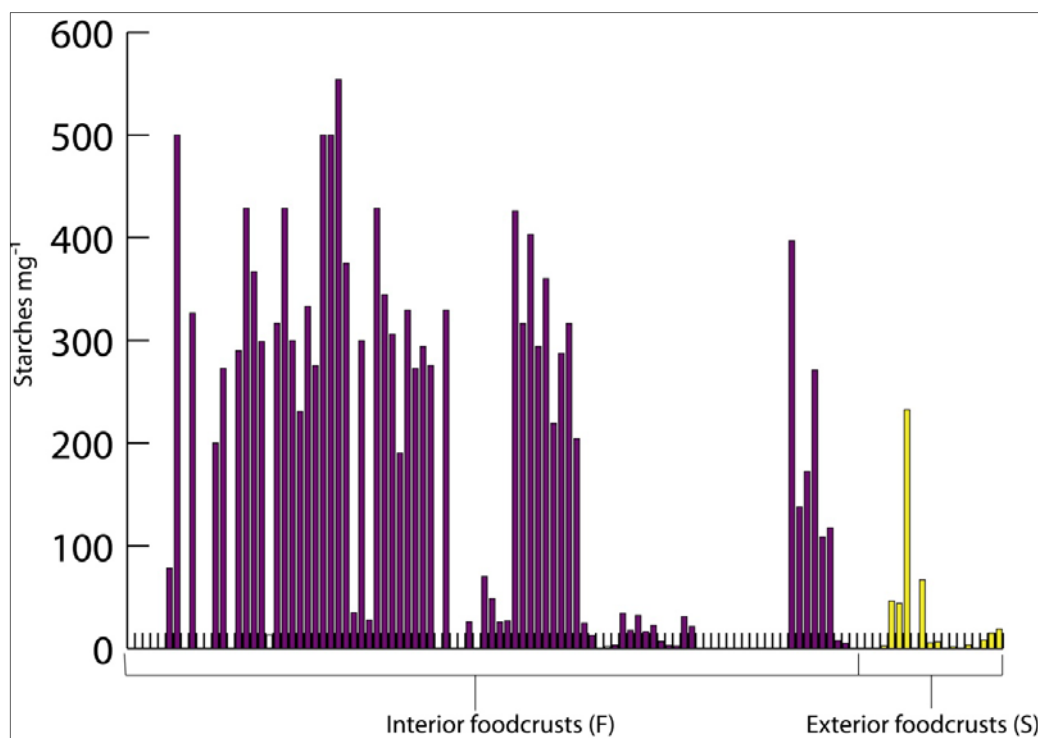
**Figure 5. 15.** Introducing the third principal component allows for the greater separation of overlapping classes, such as *Armoracia rusticana* (4) and *Sparganium erectum* (11).

## 5.6.2. Preliminary observations in the context of archaeological residues, and methodological adjustments.

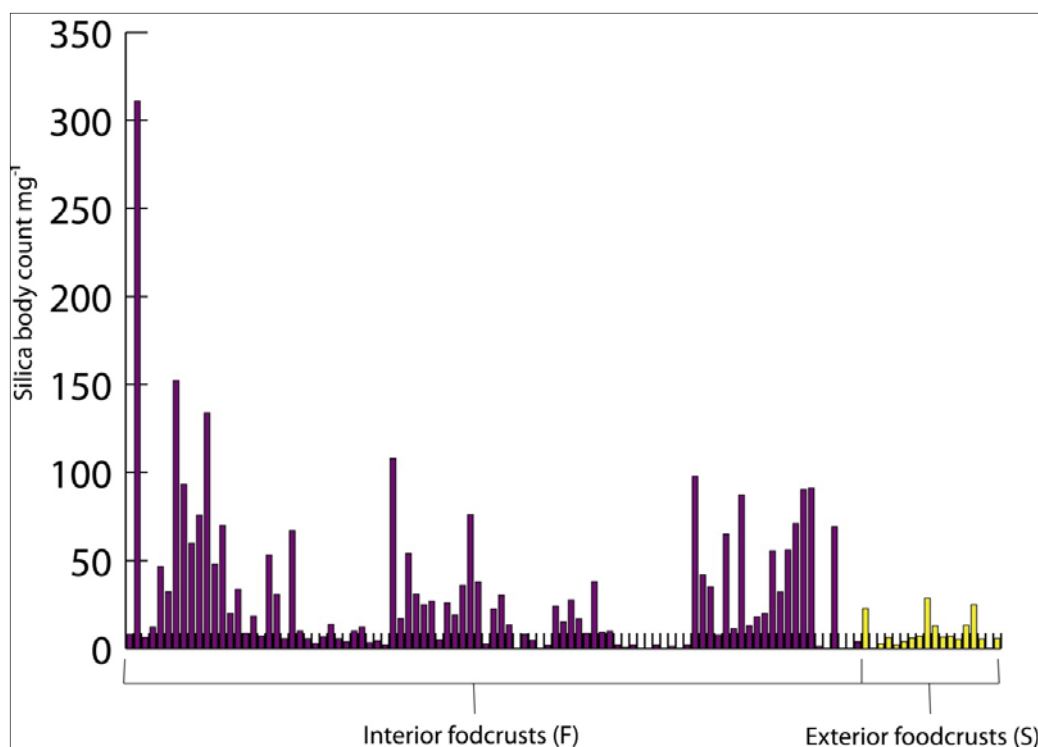
### 5.6.2.1. Ruling out contamination: collective interior versus exterior counts for all the sites.

The starch counts ( $\text{mg}^{-1}$ ) of all interior (F) and exterior (S) residues were plotted for a sum of the sites studied (figure 5.16). There is a statistical difference between the number of starch granules ( $\text{mg}^{-1}$ ) for the two ceramic surfaces (t-test,  $p=0.02$  ( $<0.05$ ),  $t=2.01$ , (F)  $N=98$ , (S)  $N=18$ ). This supports the statement that the interiors of the pots were in direct contact with starchy foods, and that in general these interior residues represent a deliberate loading with starch-rich plants. The same significant difference between (F) and (S) can be stated of silica bodies too (figure 5.17). Overall, the interior of the pots showed higher proportions ( $\text{mg}^{-1}$ ) of phytoliths, again consistent with the packing of silica-rich plant material in pots (t-test,  $p=1.46^{-05}$  ( $<0.05$ ),  $t=1.98$ , (F)  $N=98$ , (S)  $N=18$ ).





**Figure 5.16.** Counts ( $\text{mg}^{-1}$ ) of interior (F) and exterior (S) starch granules for all the sites and residues investigated.



**Figure 5.17.** Counts ( $\text{mg}^{-1}$ ) of interior (F) and exterior (S) silica bodies for all the sites and residues investigated.

It was noted that there is a considerable range in the counts  $\text{mg}^{-1}$  for both silica and starches between sites. This is due in part to preservation variation. For this reason

designating samples as ‘used for processing significant quantities of plants’, and thus forwarding them for identification analysis should be decided by intra-site statistical comparisons of interior (F) and exterior (S) counts  $\text{mg}^{-1}$ . Those that fall below site-specific counts  $\text{mg}^{-1}$  would be excluded from subsequent analysis, as they cannot be ruled out as background loading from the burial environment.

However, it was noted that on some sites where plant processing seemed to be less important overall, the small number of (F) deposits that show high counts would not be deemed viable for further investigation because they had not contributed enough to establish the (F) cluster’s significance. In this case, the small numbers of pots representing plant processing are archaeologically significant, and so it was important not to exclude them.

In cases where there was not a significant difference between (F) and (S) a less ideal measure was taken to test the significance between observationally high and low clusters. This approach not only allowed for the inclusion of those archaeologically significant samples where plants were processed on otherwise devoid sites, but it also allowed for the inclusion of a minor number of (S) deposits that had high counts. These were almost certainly the result of overspill from the interior contents of the pots, as most of these instances occur at the rim. Samples with counts  $\text{mg}^{-1}$  below a defined threshold value for that site were removed from subsequent analysis by automated classification in the case of starches, or measurement and description in the case of phytoliths.

